Materials Science and Engineering A 497 (2008) 212–215

Contents lists available at ScienceDirect

Materials Science and Engineering A

journal homepage: www.elsevier.com/locate/msea

Effects of Changes in Notch Radius and Test Temperature on the Toughness of a Nano-crystalline Aluminum Alloy Composite Produced via Extrusion of Amorphous Aluminum Alloy Powders

Hala A. Hassan[a,b,*], John. J. Lewandowski[b]

[a] Department of Design and Production Engineering, Faculty of Engineering, Ain Shams University, Cairo, Egypt
[b] Department of Materials Science and Engineering, Case Western Reserve University, Cleveland, OH, USA

ARTICLE INFO

Article history:
Received 3 June 2008
Accepted 30 June 2008

Keywords:
Nano-crystalline composites
Toughness
Temperature effects

ABSTRACT

Amorphous aluminum alloy powders were extruded to produce a nano-crystalline aluminum alloy composite-containing nano-sized particles. Significant increases to the hardness/strength were obtained via the processing-induced evolution of 35 vol.% of nano-sized particles in the aluminum matrix. Acoustic measurements of the elastic constants revealed elastic modulus (E) in the range of 86–89 GPa. The fracture toughness of these nano-structured composite materials were evaluated at room temperature and 225 °C (498 K) on fatigue-precracked samples as well as on notched samples containing different root radii. The effects of changes in the root radius and test temperature on the toughness are compared to the behavior of conventional aluminum alloys and metal–matrix composites (MMCs).

1. Introduction

Nano-crystalline metallic materials and metal–matrix composites (MMCs) both provide unique, but different combination of properties. Because of their nano-scale grain size, the nano-crystalline metallic materials typically possess high-yield strengths, as predicted by the Hall–Petch relationship [1,2] although this may not hold at the very fine grain sizes due to changes in deformation at these very fine grain sizes. MMCs have been reported to have attractive physical and mechanical properties such as high-specific modulus, good high-cycle fatigue resistance, and improved thermal stability [3–7]. Among the MMCs, particulate-reinforced MMCs are of particular interest due to their ease of fabrication, lower cost, and isotropic properties.

Combining the two concepts of MMCs and nano-crystalline materials in the form of nano-structured particulate-reinforced MMCs has the potential to provide combinations of properties not possible with conventional structural materials. For example, it has been reported that the addition of only 2 wt.% of nano-sized SiC particles improves the yield strength of as-cast aluminum alloy A356 by 50%, significantly higher than the strength improvements provided using the same amount of micrometer-sized particles [8]. Other work [9] has shown that the dispersion of 4 vol.% nano-sized Al_2O_3 particles in Al via a powder-metallurgy process doubled the yield strength. Currently, there are several fabrication methods that have been used to produce nano-structured MMCs (NMMCs), including: mechanical alloying with high-energy milling [10], ball milling [11], nano-sintering [12], vortex process [13], spray deposition, and laser deposition. However, another potential approach to produce NMMCs is via the consolidation and subsequent working of amorphous metal powders [14].

The present work was conducted in order to determine the effects of notch radius, including fatigue precracks, on the toughness of NMMCs prepared by processing-induced devitrification of amorphous Al-alloy powders. While the standard method to determine, the fracture toughness requires fatigue-precracked specimens, these specimens can require significant preparation time. Also, there are some applications where well-defined radii are present and the toughness under these conditions is needed. In the present work, both room temperature and high temperature (T = 225 °C) were studied, while testing was conducted and analyzed as done previously [15]. Comparison to conventional particulate-reinforced Al MMCs also presented [15].

2. Experimental work

2.1. Materials

Atomized $Al_{89}Ni_3Gd_7Fe_1$ powders were canned in an Al tube and extruded producing an extruded billet 15.9 mm in diameter

* Corresponding author at: Department of Design and Production Engineering, Faculty of Engineering, Ain Shams University, Cairo, Egypt.
E-mail address: halah70@yahoo.com (H.A. Hassan).

0921-5093/$ – see front matter © 2008 Elsevier B.V. All rights reserved.
doi:10.1016/j.msea.2008.06.048

with a 2 mm-thickness Al layer on the outside. An extrusion ratio of 20:1 was used at 673 K. Hot extrusion of the amorphous powders results in the formation of an ultra-fine structure consisting of roughly 35 vol% of nano-structured intermetallic particles (e.g. 100 nm-thick), in an aluminum matrix [27]. Elastic constants were measured using acoustic techniques and revealed Young's modulus (E) in the range 86–89 GPa.

2.2. Specimen preparation

As-extruded bars were machined using electro-discharge machining (EDM) into rectangular beams with a cross-section of 5 mm × 10 mm eventual for three-point bend (3PB) testing. Toughness tests were conducted in three-point bending for both notched and precracked samples. The notches were produced either by grinding (i.e. $\rho = 450\,\mu m$) or by using a low speed well vertical diamond impregnated wire saw (i.e. $\rho = 100\,\mu m$). The fatigue precracks were placed in general accordance with ASTM standard E647-2000 [16]. All the notches and precracks were placed to a depth of a/w = 0.5 according to the standards [17].

2.3. Testing procedure

The toughness tests were carried out on a 20 Kip MTS closed loop servohydraulic machine using a MTS 458.20 controller, with FTA control software. Fatigue precrack length was measured using 5 mm metallic foil KRAK© (KG-A05)-gages, monitored by a Fractomat model 1288 crack measurement system. During fatigue precracking, crack growth was measured at a frequency of 20 Hz, load ratio of 0.1 under decreasing ΔK conditions (ΔK-control), using an automated load-shedding technique. The fracture toughness tests were carried out under displacement rate control of 0.5 mm/min. The toughness tests were monitored and recorded by LABVIEW program. The high-temperature tests were conducted inside an ATS model controlled temperature cabinet with a temperature control to within ±1 °C using a MTS 409.8 temperature controller. After reaching the test temperature inside the chamber, the specimens were held for 30 min to equilibrate prior to starting the test. Load and temperature are monitored in addition to crack length via KRAK gages.

2.4. Fracture surface analysis

Fractured samples were examined using Philips XL30 or Hitachi S-4500 high-resolution SEM both operated at 15 KV.

3. Results

Table 1 summarizes the values for toughness (K_Q and K_{IC}) at catastrophic fracture as a function of the notch root radius for all the specimens tested at RT and 225 °C (498 K) while Fig. 1 plots the data. The toughness at room temperature increased on going from a fatigue precrack to 450 μm notch root radius. A similar trend, but less in magnitude was exhibited at 225 °C (498 K). Fig. 2 summarizes the effects of changes in test temperature on the toughness values obtained for fatigue-precracked and notched samples. Increasing the test temperature increased the toughness for both the fatigue-precracked and notched samples containing the 100 μm notch. In contrast, increasing the test temperature reduced the notch toughness for samples with the 450 μm notch.

Typical high-resolution SEM fractography for fatigue-precracked samples tested at room temperature are given in Fig. 3. Samples containing 450 μm notches exhibited similar fractography. The fracture surfaces contained dimpled fracture with dimple sizes on the order of 0.49 ± 0.18 μm for fatigue-precracked samples and 0.42 ± 0.10 μm for samples with the 450 μm notches. Examination of the dimples at high magnification revealed that each dimple contained multiple nuclei/particles (Fig. 3).

Table 1
Effects of notch radius and test temperature on the fracture toughness K_{IC} and K_Q

Test temperature (°C) (K)	Materials	K_{IC} and K_Q (MPa m$^{1/2}$)		
		Notch root radius ρ		
		0 μm	100 μm	450 μm
25 (298 K)	32-B	9	26.8	40
	40-B	5.6	27.6	45
	41-B	9	30	49
225 (498 K)	32-B	16.5	31	N/A
	40-B	12.5	29.7	34
	41-B	23.3	33	39.5

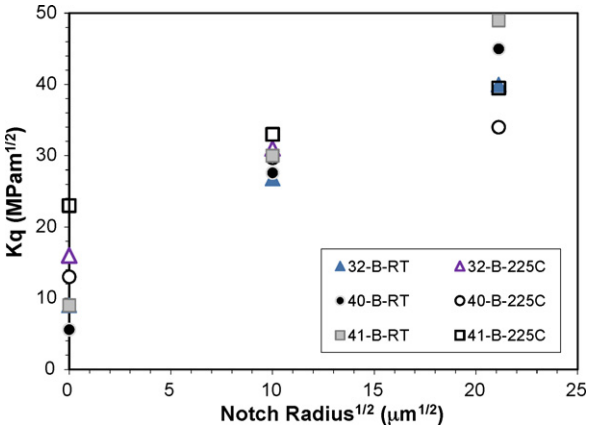

Fig. 1. The effect of changes in notch root radius on the fracture toughness (K_Q) of the nano-structured aluminum composite at room temperature (closed symbols) and 225 °C (498 K) (open symbols).

4. Discussion

An increase in toughness with increase in notch radius has been documented on many materials systems [18–20], including MMCs [15]. The fatigue-precracked samples tested at both room temperature and 225 °C (498 K) can be considered as valid plane strain

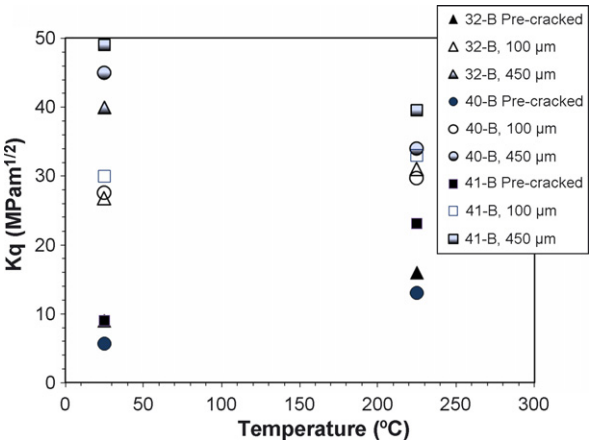

Fig. 2. The effect of changes in test temperature on the fracture toughness (K_Q) obtained for fatigue-precracked (closed symbols) and notched samples, for notched radii 100 μm (open symbols), and 450 μm (half-filled symbols).

Table 2
Summary of the plastic zone sizes at the initiation of stable crack growth K_i and at the overload K_{IC}, and the critical thickness for each sample according to ASTM E399 [17] for tests at 225 °C (498 K)

ID	K_i (MPa m$^{1/2}$)	r_p (ε) (mm)	r_p (σ) (mm)	K_{IC} (MPa m$^{1/2}$)	r_p (ε) (mm)	r_p (σ) (mm)	B_{crit} (mm)
32-5B	9	0.014	0.043	16.5	0.05	0.143	2.3
40-6B	11	0.021	0.064	12.5	0.03	0.082	1.3
41-6B	10.7	0.020	0.060	23.3	0.10	0.286	4.5

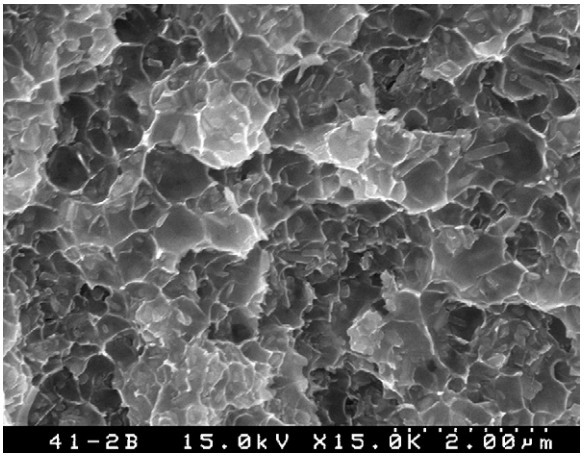

Fig. 3. SEM image for (41-2B) nano-structured Al composite fatigue-precracked at RT.

fracture toughness, K_{IC}, as the calculated plastic zone sizes (e.g. $r_p = 70\ \mu m < B/50$, where B = sample thickness) are well within the ASTM standards and the sample thickness exceed that required for a valid K_{IC} (Table 2). Samples tested at room temperature all failed without stable crack growth in contrast to samples tested at 225 °C (498 K) that exhibited stable crack growth. Table 2 summarizes both the K at fracture initiation, K_i, as well as K_{IC} for these cases.

The trend of these results are similar to previous work [15] on MB78/SiC/20p MMC containing 15 μm average size SiC_p in both underaged (UA) and overaged (OA) conditions, where a linear relation between K_Q and $\rho^{1/2}$ was reported for both cases until reaching a limiting value of notch root radius. Fig. 4 summarizes the present data along with previous work [15] on particulate-reinforced MMCs containing 15 vol.% of 15 μm average size SiC particulates. In those early works on particulate-reinforced MMCs [15,21–23], the Rice and Johnson model [24] of ductile fracture toughness was utilized to rationalize the differences in toughness obtained with different volume fraction and/or size of reinforcement for composites containing up to 20 vol.% reinforcement and particle sizes ranging from 3 to 50 μm. In this model all particles are considered to crack or decohere ahead of the major crack tip and at low strain. The regions of plastic flow are limited to a volume of width "d" which corresponds to interparticle spacing, where $\delta = J_{IC}/\sigma_f$. For a homogenous arrangement of particles, the interparticle spacing (λ) can be estimated using the following relation [25]:

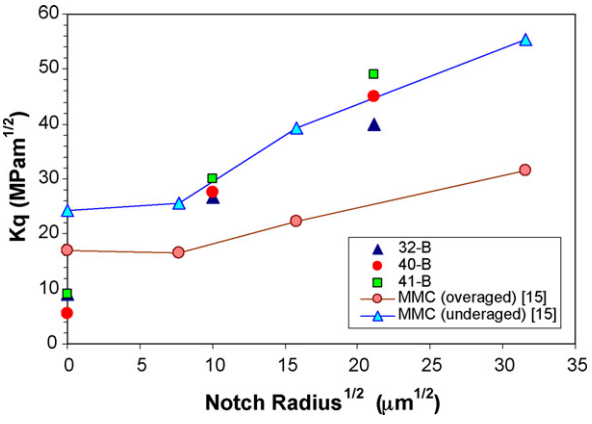

Fig. 4. Comparison between the effect of notch root radius on the fracture (K_Q) of the nano-structured aluminum composite and previous work [15] on MMC at RT.

$$\lambda = 0.77 d v^{-1/2}$$

where d is the average particle size and v is the volume faction of the reinforcement.

The present materials contain roughly 35 vol.% of fine (e.g. 100 nm-thick) intermetallics that have been shown to decrease the grain size while increasing the modulus to 86–89 GPa. If the particles in the nano-structured alloy are uniformly distributed in the aluminum matrix, an interparticle spacing of roughly 0.13 μm is calculated. Assuming that the Rice and Johnson model [24] can be used in such a situation indicates that the critical crack opening displacement calculated as $CTOD = 0.49 K^2/\sigma_y E$, should be on the order of the interparticle spacing for fracture link-up to occur (i.e. $\lambda = \delta$). The predicted δ_{crit} for each fatigue-precracked sample is provided in Table 3, using data for yield strength consistent with previous work on similar materials [27]. Also included in Table 3 are calculated critical crack opening displacements for each of the fatigue-precracked samples. The predicted δ_{crit} is below the experimental results for CTOD obtained presently. The disagreement between the experimental data and that predicted by the Rice and Johnson model [24] likely results from differences in the effective particle spacing for the nucleation of cavities ahead of the fatigue precrack tip. The Rice and Johnson model [24] assumes uniformly distributed particles with the requirements that each particle participates in the fracture process and creates one dimple on the fracture surface. This approach works reasonably well when applied to a variety of particle-containing materials when the volume fraction is low [26] as well as to some particulate-reinforced MMCs containing less than 20 vol.% of μm sized particulates [15,23], as each particle/reinforcement particle in those studies typically were associated with one dimple on the fracture surface. However, in the present case, SEM analyses reveal that multiple particles were present in each dimple on the fracture surface (cf. Fig. 3), suggesting that clusters of nano-sized particles each nucleate a dimple, thereby increasing the effective spacing of cavity-nucleating features (i.e. clustered nano-particles). If one assumes that four to seven particles are present in each dimple, consistent with fracture surface observations, the effective interparticle spacing (λ) increases from 0.13 μm to 0.5–0.9 μm, somewhat closer to the experimental data obtained presently (Table 3). Fracture surface observations suggest that the nano-sized particles debond from the matrix as no evidence of cracked particles was found.

Increasing the test temperature was shown to increase the toughness for the fatigue-precracked samples and those containing 100 μm notches, although samples containing the 450 μm notches showed a reduced notch toughness on going from room

Table 3
Summary of the calculated and measured parameters from SEM fractography

ID	Conditions	K_{IC} (MPa m$^{1/2}$)	CTOD (δ) (μm)	$\delta_{crit} = \lambda^*$ (μm)	Dimple size (μm)	No. of particles/dimple
41-2B	Precracked, RT (298 K)	9	0.7	0.13	0.49 ± 0.18	2.5 ± 1.5
41-6B	Precracked, 225 °C (498 K)	23.3	5.4	0.13	0.80 ± 0.2	4.0 ± 3.0

temperature to 225 °C (498 K). In the case of increasing toughness obtained on the fatigue-precracked samples tested at room temperature and 225 °C (498 K), fracture surface observations of the fatigue-precracked toughness tests conducted at 225 °C (498 K) showed 0.8 ± 0.2 μm dimple sizes with up to seven particles in each dimple (Table 3). Although the calculation of CTOD (δ) at $K_{max} = K_{IC}$ is 5.4 μm, when the initiation toughness of 10.7 MPa m$^{1/2}$ is used to calculate CTOD (δ) this value reduces to 1.15 μm. Interestingly, the present samples do not undergo a drop in toughness at intermediate test temperatures like that often exhibited in dispersion strengthened aluminum alloys or other nano-crystalline systems, [27], at least at the loading rates presently used.

5. Conclusions

Processing-induced devitrification of amorphous aluminum alloy powder has been used to produce nano-crystalline composite materials with increased hardness, elastic modulus and toughness. The effects of changes in notch radius and test temperature on the toughness were generally consistent with previous work on particulate-reinforced MMCs where increases in notch radius produced increased values for toughness. However, fracture surface features revealed the participation of the multiple nano-sized particles in the formation of one dimple on the fracture surface. Predications of the critical crack opening displacement for fracture were consistent with such observations.

Acknowledgements

The authors thank DARPA/SAM program for providing financial support and acknowledge interactions with Drs. Tom Watson and Martin Blackurn of Pratt and Whitney Company. HAH also acknowledges the support of a Fulbright Scholarship for her work at CWRU and the assistance of Dr. D. Li for SEM.

References

[1] E.O. Hall, Proc. Phys. Soc. Lond. Sec. B 64 (1951) 747–753.
[2] N.J. Petch, J. Iron Steel Inst. 174 (1953) 25–28.
[3] T.W. Clyne, P.J. Withers, An Introduction to Metal Matrix Composites, Cambridge University Press, New York, 1995.
[4] S.C. Tjong, Z.Y. Ma, Mater. Sci. Eng. R 29 (2000) 49–113.
[5] D.S. Liu, M. Manoharan, J.J. Lewandowski, Metall. Trans. A 20 (11) (1989) 2409–2417.
[6] A.R. Vaidya, J.J. Lewandowski, Mater. Sci. Eng. A 220 (1/2) (1996) 85–92.
[7] D.S. Liu, J.J. Lewandowski, Metall. Trans. A 24 (3) (1993) 609–615.
[8] Y. Yang, J. Lan, X. Li, Mater. Sci. Eng. A 380 (2004) 378–383.
[9] Y.C. Kang, S.L. Chan, Mater. Chem. Phys. 85 (2004) 438–443.
[10] X.F. Chen, E.G. Baburai, F.H. Froes, A. Vassel, Proc. Adv. Mater. Processes (1997) 185–192.
[11] S.L. Urtiga Filho, R. Rodriguez, J.C. Earthman, E.J. Lavernia, Mater. Sci. Forum 416–418 (2003) 213–218.
[12] J.R. Groza, Int. J. Powder Metall. 35 (1999) 59–66.
[13] K. Akio, O. Atsushi, K. Toshiro, T. Hiroyuki, J. Jpn. Inst. Light Metal 49 (1999) 149–154.
[14] D.V. Louzguine-Luzgin, A. Inoue, J. Nanosci. Nanotechnol. 5 (7) (2005) 999–1014.
[15] M. Manoharan, J.J. Lewandowski, Int. J. Fract. 40 (1989) R31–R34.
[16] ASTM E647, Standard Test Method for Measurement of Fatigue Crack Growth Rates, ASTM, Philadelphia, PA, 2000.
[17] ASTM E399-2000, standard test method for plane strain fracture toughness of metallic materials, American Society for Testing and Materials, Philadelphia, PA, 2000.
[18] J.J. Lewandowski, Mater. Trans. JIM 42 (4) (2001) 633–637.
[19] J.J. Lewandowski, M. Shazly, A.S. Nouri, Scripta Mater. 54 (3) (2006) 337–341.
[20] J.F. Knott, Fundamentals of Fracture Mechanics, Butterworths, London, 1973.
[21] S.V. Kamat, J.P. Hirth, R. Mehrabian, Acta Metall. 37 (1989) 2395–2402.
[22] M. Manoharan, J.J. Lewandowski, Acta Metall. 38 (1990) 489–496.
[23] M. Manoharan, J.J. Lewandowski, Mater. Sci. Eng. A 150 (1992) 179–186.
[24] J.R. Rice, M.A. Johnson, in: M.F. Kanninen, H. Liholt, O.B. Pedersen (Eds.), Inelastic Behavior of Solids, McGraw-Hill, New York, NY, 1969, p. 641.
[25] G. LeRoy, J.D. Embury, G. Edwards, M.F. Ashby, Acta Metall. 29 (1981) 1509–1522.
[26] W.M. Garrison Jr., N.R. Moody, J. Phys. Chem. Solids 48 (11) (1987) 1035–1074.
[27] X.L. Shi, R.S. Mishra, T.J. Watson, Scripta Mater. 25 (2005) 887–891.